Radio-frequency transitions on weakly bound ultracold molecules

Cheng Chin[1,*] and Paul S. Julienne[2]
[1]*Institut für Experimentalphysik, Universität Innsbruck, Technikerstrasse 25, 6020 Innsbruck, Austria*
[2]*Atomic Physics Division, National Institute of Standards and Technology, 100 Bureau Drive Stop 8423, Gaithersburg, Maryland 20899, USA*
(Received 21 August 2004; published 27 January 2005)

We show that radio-frequency spectroscopy on weakly bound molecules is a powerful and sensitive tool to probe molecular energy structure as well as atomic scattering properties. An analytic expression of the excitation line shape is derived, which in general contains a bound-free component and a bound-bound component. In particular, we show that the bound-free process strongly depends on the sign of the scattering length in the outgoing channel and acquires a Fano-type profile near a Feshbach resonance. The derived line shapes provide an excellent fit to both numerical calculations and recent experimental measurements based on $^6Li_2$.

DOI: 10.1103/PhysRevA.71.012713 PACS number(s): 34.50.−s, 03.75.Hh, 05.30.Fk, 39.25.+k

I. INTRODUCTION

Radio-frequency (rf) spectroscopy is widely applied to many experiments on atoms or molecules, for which an exquisite energy resolution can reveal the interactions and dynamics of the constituents. In recent experiments on ultracold weakly bound molecules, rf spectroscopy also allowed a precise determination of the molecular binding energy [1,2] and the pairing gap in a degenerate Fermi gas [2]. In the latter case, the high-energy resolution reveals the fermionic nature of the pairing in the Bose-Einstein condensation (BEC) to Bardeen-Cooper-Schreiffer state (BCS) crossover regime.

In this article, we show that much more information regarding the atomic interaction properties can be extracted from the rf spectroscopy of ultracold molecules (BEC regime). Based on the scattering theory in the threshold regime, we derive simple analytic formulas for the rf excitation rates and their line shapes. Our calculations confirm the characteristic broad and asymmetric bound-free dissociation spectra observed in Refs. [1,2], from which one can precisely determine the atomic scattering lengths as well as the molecular binding energy. Furthermore, we show that in the presence of a Feshbach resonance in the final scattering channel, the spectra will develop into two components: a bound-bound transition to the newly formed molecular state and a remaining weaker bound-free transition. Our results provide excellent fits to both numerical calculations and the experimental measurements on the $^6Li_2$ molecules [2,3].

We would like to point out that, compared to photoassociation spectroscopy [4,5] and collision rate measurements, rf spectroscopy on weakly bound molecules provides several advantageous features in probing the scattering properties of ultracold atoms. First of all, rf transitions in the ground-state manifold are highly precise since Doppler effects and recoil shifts are negligible; sub-kHz frequency resolution is expected [3]. Second, unlike the free-bound transitions of photoassociation spectroscopy and the collision rate measurements, our rf bound-free or bound-bound transitions start from bound molecules, do not require any collision or thermalization process, and have the same efficiency regardless of the sample density. Whereas two-color photoassociation spectroscopy is useful in locating bound molecular states with binding energies on the order of 1 GHz or more [6], rf spectroscopy can probe very weakly bound states with binding energies less than 1 MHz. Finally, rf transitions can be used to study collision properties in different scattering channels by driving the rf transitions to the relevant quantum states.

In this paper, we first introduce our model and derive the excitation line shape (Sec. II). We then compare our result to the numerical calculation (Sec. III) and discuss the spectral features (Sec. IV). Finally, we compare our results to the experiment (Sec. V).

II. MODEL

We consider a weakly bound molecule in the state $|m\rangle$. The bound state consists of two atoms at energy $-E_b = -\hbar^2/2\mu(a-r_0)^2$ below the dissociation continuum A [7], where $E_b > 0$ is the binding energy. Here $\hbar$ is Planck's constant h divided by 2π, μ is the reduced mass of the two atoms, a is the scattering length in the scattering channel A, and r_0 is the interaction range of the van der Waals potential [7], which varies with interatomic separation r as $-C_6/r^6$,

$$r_0 = 2^{-3/2}\frac{\Gamma\left(\frac{3}{4}\right)}{\Gamma\left(\frac{5}{4}\right)}\left(\frac{2\mu C_6}{\hbar^2}\right)^{1/4}. \quad (1)$$

For weakly bound molecules, we assume $a \gg r_0 > 0$. The molecule is initially at rest and a radio-frequency photon with energy $E_{\rm rf}$ couples the molecule to a different channel A', characterized by the scattering length a'. For $a' < 0$, the final state is a continuum and the excited molecule dissociates; for $a' > 0$, a weakly bound state $|m'\rangle$ is also available in the final-state channel A' and the rf can either dissociate the molecule or drive it to the bound state $|m'\rangle$. In the following, we assume that both scattering channels are in the threshold

*Present address: Department of Physics and James Franck Institute, University of Chicago, Chicago, IL 60637, USA.

regime ($a, |a'| \gg r_0$). Atoms, bound or unbound, then have the same internal wave function. We also assume the relative energy of the continuum threshold to be $E_{A'} - E_A = E_0 > 0$ and that the bound states $|m\rangle$ or $|m'\rangle$ do not decay on the time scale of an rf experiment.

A. Bound-free transition

Here we consider the bound-free transition of a stationary molecule. Energy conservation gives

$$E_{\rm rf} = E_0 + E_b + K, \tag{2}$$

where $K = \hbar^2 k^2 / 2\mu > 0$ is the kinetic energy of the outgoing wave and k is the associated wave number. For $E_{\rm rf} < E_0 + E_b$, the transition is forbidden. For $E_{\rm rf} \geqslant E_0 + E_b$, the bound-free transition rate from the initial state $|m\rangle$ to the final state $|K\rangle$ is given by Fermi's golden rule,

$$\Gamma_f(K) = \frac{2\pi}{\hbar} \left| \left\langle K \left| \frac{\hbar\hat{\Omega}}{2} \right| m \right\rangle \right|^2 = \frac{h\Omega^2}{2} F_f(K), \tag{3}$$

where

$$F_f(K) = \left| \int \psi_K^*(r) \phi_m(r) dr \right|^2 \tag{4}$$

is the bound-free Franck-Condon factor per unit energy, $\hbar\hat{\Omega}/2$ is the rf interaction for the rf Rabi frequency Ω, $\phi_m(r)$ is the bound molecular wave function in channel A, and $\psi_K(r)$ is the energy-normalized s-wave scattering wave function in channel A' [8].

A bound-free Franck-Condon factor similar to that in Eq. (4) also occurs in the theory of photoassociation line shapes [9], with optical dipole coupling replacing the rf coupling matrix element. While such Franck-Condon factors generally need to be evaluated numerically [10], we can evaluate the bound-free Franck-Condon factor for our assumed case based solely on the asymptotic behavior of the bound and scattering wave functions,

$$\psi_K(r) = \sqrt{\frac{2\mu}{\pi\hbar^2 k}} \sin(kr + \delta'), \tag{5}$$

$$\phi_m(r) = \sqrt{\frac{2}{a}} e^{-r/a}, \tag{6}$$

where δ' is the scattering phase shift in channel A'. Combining Eqs. (4)–(6), we have

$$F_f(K) = \frac{4\mu a}{\pi\hbar^2 k} (1 + k^2 a^2)^{-2} (\sin\delta' + ka\cos\delta')^2. \tag{7}$$

Since $k \ll 1/r_0$, we can use the low-energy expansion of the scattering phase shift [11],

$$k\cot\delta' = -\frac{1}{a'} + \frac{r_e'}{2} k^2 + O(k^4), \tag{8}$$

where the effective range r_e' depends on the scattering length a' and the interaction range r_0. The explicit form of r_e' for a van der Waals potential is given in Ref. [12] in the limit $|a'| \gg r_0$,

$$r_e' = \frac{\Gamma\left(\frac{1}{4}\right)^4}{6\pi^2} r_0. \tag{9}$$

By taking the leading term in the expansion in Eq. (8) and expressing $k^2 a^2 = K/E_b$ and $k^2 a'^2 = K/E_b'$, we derive a simple and very useful form of the line shape,

$$F_f(K) = \frac{2}{\pi} \left(1 - \frac{a'}{a}\right)^2 \frac{K^{1/2} E_b^{1/2} E_b'}{(K + E_b)^2 (K + E_b')}. \tag{10}$$

In the limit $k \to 0$, where $\delta' = -ka'$, we have $F_f \sim K^{1/2}$, which is expected in the Wigner threshold regime. The transition rate peaks between $K \sim 0$ for $|a'| \gg a$ and $K = E_b/3$ for $|a'| \ll a$ and decreases to higher K. For very large $K \gg \hbar^2/m r_0^2$, Eq. (8) is no longer valid. A few extreme situations, including $a = a'$, where F_f vanishes, $a' = \pm\infty$, and the Wigner threshold law fails, will be discussed in later sections.

The integrated rf line strength S_f is given by

$$S_f = \int_0^\infty F_f(K) dK \tag{11}$$

$$= \begin{cases} 1 & \text{for } a' \leqslant 0 \\ \left(\frac{a - a'}{a + a'}\right)^2 & \text{for } a' > 0. \end{cases} \tag{12}$$

The unit value of S_f for $a' < 0$ means that within the approximations we made, the scattering states $|K\rangle$ provide a complete set of final states for the rf transition. In contrast, $S_f < 1$ when $a' > 0$, and the scattering states no longer provide completeness. This is due to an additional bound state that exists in the final-state channel A' when $a' > 0$. The bound state allows a new bound-bound transition process.

B. Bound-bound transition

For positive scattering length in the outgoing channel $a' \gg r_0 > 0$, a weakly bound molecular state $|m'\rangle$ exists. Bound-bound transitions are allowed. From energy conservation, we have

$$E_{\rm rf} = E_0 + E_b - E_b', \tag{13}$$

Effectively, $K = -E_b'$. The bound-bound Franck-Condon factor $F_b(K)$ can be calculated similar to Eqs. (3) and (4),

$$F_b(K) = \left| \int \phi_{m'}^*(r) \phi_m(r) dr \right|^2 \delta(K + E_b') \tag{14}$$

$$= \frac{4aa'}{(a + a')^2} \delta(K + E_b'), \tag{15}$$

where we have used the molecular wave function in Eq. (6) for both $|m\rangle$ and $|m'\rangle$ states and have introduced the δ function to provide energy normalization analogous to that of $F_f(K)$. The bound-bound line strength is then $S_b = 4aa'/(a + a')^2$.

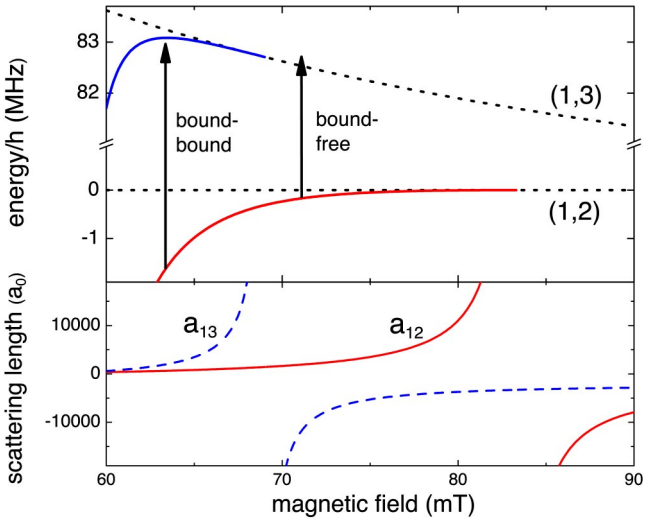

FIG. 1. Energy structure and the scattering lengths of $^6Li_2$ in the (1,3) and (1,2) channels (dotted lines) vs magnetic field. All energies are referenced to the (1,2) scattering threshold. In these two channels, Feshbach couplings induce the formation of molecules (solid lines) below 69.0 mT and 83.4 mT, respectively. Arrows show the bound-bound and bound-free transitions based on molecules in the (1,2) channel. The lower figure shows the scattering lengths in the two channels in units of Bohr radius a_0.

Note that sum of the bound-bound and bound-free integrated line strengths is identically 1 for $a' > 0$,

$$S_f + S_b = 1, \tag{16}$$

as expected from the wave-function projection theorem.

III. COMPARISON WITH NUMERICAL CALCULATION

We check the validity of the above analytic formulas by comparing them to a numerical calculation. We choose fermionic ^{6}Li atoms as our model system, for which the interaction parameters are precisely known by fitting various cold atom and molecule measurements to a multichannel quantum scattering calculation. The energy structure and the scattering lengths in the two relevant channels $A=(1,2)$ and $A'=(1,3)$ are shown in Fig. 1. Here, (1,2) refers to the state with one atom in state $|1\rangle$ and one in $|2\rangle$, and $|N\rangle$ refers to the lowest Nth internal state in the ^{6}Li atom ground-state manifold, having respective total spin projection quantum numbers of $1/2$, $-1/2$, and $-3/2$ (see Ref. [13]).

To calculate the scattering phase shifts versus collision energy, we construct a single-channel Hamiltonian to describe the (1,3) continuum. The single-channel potential is selected to have the identical scattering length and van der Waals coefficient as the full multichannel model. The phase shifts from this model are nearly indistinguishable from those obtained from the full multichannel calculations in this range of magnetic fields. The van der Waals interaction is set to $C_6=1393.39(16)$ a.u. [14] (1 a.u.$=9.573\,44\times10^{-26}$ J nm^6), yielding an interaction range of $r_0=29.884(3)a_0$ (Bohr radius $a_0=0.052\,917\,7$ nm). Figure 2 compares the scattering phase shifts from the numerical calculation with those from the effective range expansion given in Eq. (8). Here, the scattering parameters are based on the (1,3) scattering states at 72.4 mT with a scattering length of $a'=-7866a_0$. The result shows the expected behavior that $k\cot\delta'=-1/a'$ provides an excellent fit at low scattering energy, $K/k_B<20$ μK, and the effective range correction works up to $K/k_B\approx10$ mK (k_B is Boltzmann's constant).

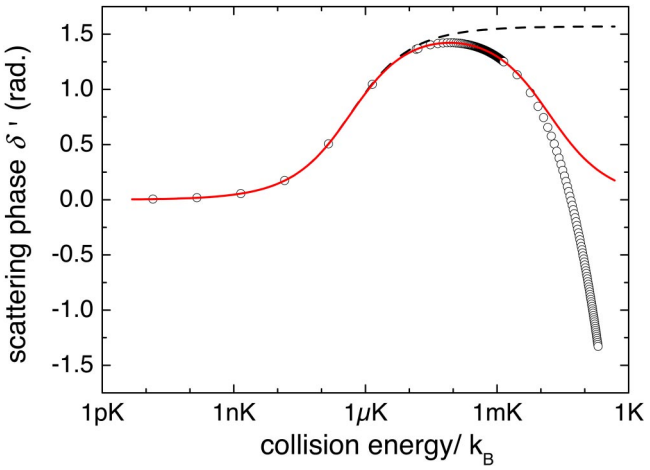

FIG. 2. Scattering phase shifts vs collision energy. The numerical calculation (open circles) is shown together with the predictions from Eq. (8) with (solid line) and without (dashed line) the effective range correction. The scattering parameters are based on ^{6}Li in the (1,3) channel near 72.4 mT with $a_{13}=-7866a_0$.

We also compare the Franck-Condon factors obtained from the numerical calculation and from Eq. (10). The numerical calculation is based on an initial bound state in the (1,2) channel and the final-state (1,3) continuum, described by the reduced Hamiltonian. We show the calculations at two

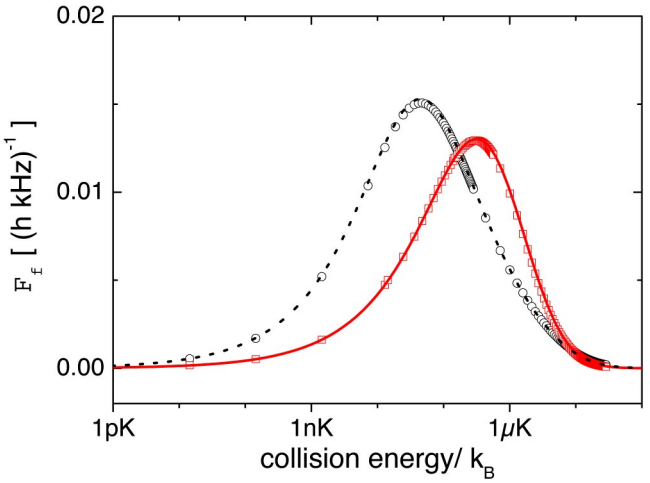

FIG. 3. Comparison of the Franck-Condon factors from numerical calculation and from theory. Numerical calculation at 72.4 mT (open squares) and 68.2 mT (open circles) are plotted together with the formula Eq. (10) (solid line at 72.4 mT and dotted line at 68.2 mT). The parameters are $E_b/k_B=16.2$ μK and $a'=25173a_0$ at 68.2 mT; $E_b/k_B=6.2$ μK and $a'=-7866a_0$ at 72.4 mT.

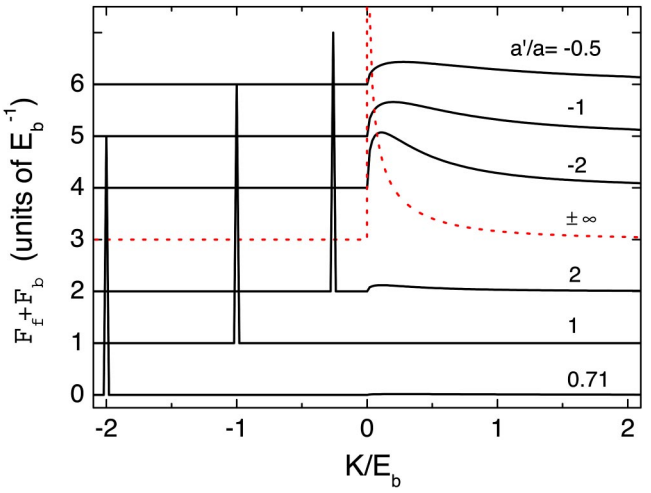

FIG. 4. Transition from a bound-free spectrum to a bound-bound spectrum. The Franck-Condon factors are calculated based on Eq. (10) and Eq. (15). Curves of different a'/a are offset and shown in the order of that near a Feshbach resonance in the A' dissociation channel (dotted line for the resonance condition). For $a'>0$, the locations of the bound-bound transitions are indicated by the sharp peaks. Notably, the bound-free transition vanishes at $a'=a$.

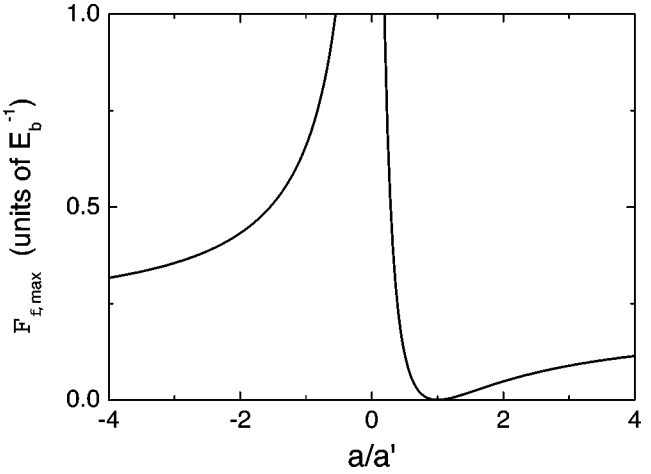

FIG. 5. Fano profile near a Feshbach resonance in the outgoing dissociation channel A'. The peak Franck-Condon factors $F_{f,\max}$ are calculated for different a/a' based on Eq. (10). Near the Feshbach resonance, a/a' approaches zero and $F_{f,\max}$ diverges.

magnetic fields of 72.4 mT and 68.2 mT, where the scattering parameters are set according to the multichannel calculations. The results show that Eq. (10) provides excellent fits to the full bound-free spectra (see Fig. 3).

IV. rf LINE SHAPE NEAR A FESHBACH RESONANCE

The appearance of the bound-bound transition for only $a'>0$ seems to suggest a distinct behavior in rf excitation near the Feshbach resonance where the scattering length changes sign. In this section, we show that the evolution of the rf spectrum is actually continuous when the magnetic field is tuned through the resonance position. We use Eq. (10) and Eq. (15) to show the bound-free and bound-bound spectra in the vicinity of a Feshbach resonance.

Figure 4 shows a continuous change near a Feshbach resonance from a bound-free line shape for $a'<0$ to a combination of bound-bound and bound-free transitions for $a'>0$. When the scattering length approaches negative infinity, the linewidth of the bound-free line shape approaches zero as $\sim E_{b'}^2 \sim a'^{-4}$ and "evolves" into the bound-bound δ function. Remarkably, for $a'>0$, the bound-free transition is much weaker. At $a'=a$, the bound-free transition is fully suppressed, $\Gamma_f=0$.

The vanishing bound-free transition for $a'\approx a$ can be understood by the wave-function overlap given in Eq. (4). As a positive scattering length a' indicates a zero in wave function near $r\approx a$, the sign change of the scattering wave function results in a cancellation in the overlap. Alternatively, we may consider that the transition amplitude to the continuum A' is exactly canceled by the Feshbach coupling between the molecular state $|m'\rangle$ and the continuum A'. This interference effect results in the Fano-like profile of the peak bound-free transition rate near a Feshbach resonance [15] (see Fig. 5). On the other hand, the bound-bound Franck-Condon factor approaches 1 when $a'\approx a$, since both molecular wave functions are identical for $r>r_0$.

Based on the above features, the rf spectroscopy does provide a new strategy to extract various important scattering parameters. In particular, while collision rate measurements are generally insensitive to the sign of the scattering length, our rf excitation spectroscopy is drastically different for the two cases and provides a new tool to probe the scattering properties.

V. COMPARISON WITH EXPERIMENT

We take the recent ^{6}Li experiment as a model system and calculate the rf spectra. The experimental spectra are obtained from the Li group in Innsbruck.

Adopting the convention used in Ref. [2], we define the rf offset energy as $E=E_{\rm rf}-E_0=K+E_b$. Using Eqs. (10) and (15), we can rewrite the Franck-Condon factors as

$$F_f(E)=\frac{2}{\pi}\left(1-\frac{a'}{a}\right)^2\frac{E_b'E_b^{1/2}(E-E_b)^{1/2}}{E^2(E+E_b'-E_b)}, \qquad (17)$$

$$F_b(E)=\frac{4aa'}{a+a'}\delta(E-E_b+E_b') \text{ for } a'>0. \qquad (18)$$

We compare the theoretical calculation with the measurement at different magnetic fields, shown in Fig. 6. For the theoretical curves, we adopt the scattering lengths and the binding energies in the initial channel $A=(1,2)$ and the final channel $A'=(1,3)$ from a multichannel calculation [16]. Their values and the magnetic-field dependence are shown in Fig. 1.

The evolution of the rf excitation line shape in the magnetic-field range of 66 mT to 76 mT (Fig. 6) shows sev-

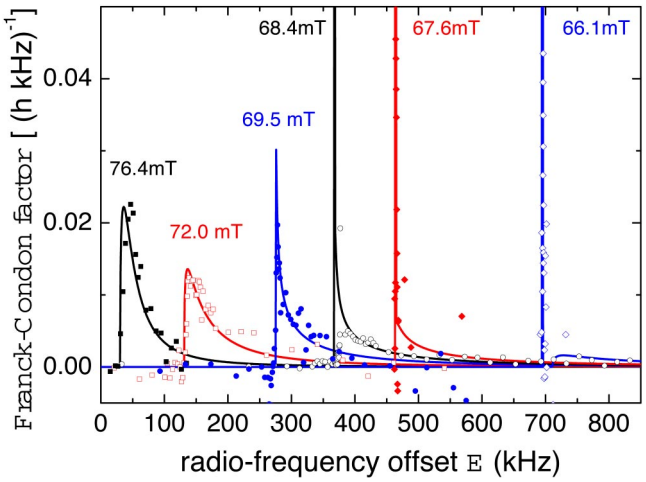

FIG. 6. rf spectra of $^6Li_2$ molecule at different magnetic field values. Theoretical curves are based on Eq. (17) and Eq. (18) with the binding energies and scattering lengths obtained from the multichannel calculation. rf-induced loss on the molecular population at 76.4 mT (solid squares), 72.0 mT (open squares), 69.5 mT (solid circles), 68.4 mT (open circles), 67.6 mT (solid diamonds), and 66.1 mT (open diamonds) is rescaled. Experiment data are from Grimm's Li group in Innsbruck [3].

eral interesting features due to the changes of the underlying molecular energy structure. When the magnetic field approaches 69.0 mT from higher values, the molecular binding energy E_b in the (1,2) channel increases (see Fig. 1). This dependence is shown in Fig. 6 as the whole excitation line moves toward higher frequency when the magnetic field decreases. At the same time, the line shape becomes sharper due to the emergence of a Feshbach resonance in the (1,3) channel at 69.0 mT. Below 69.0 mT, we expect both bound-free and bound-bound transitions to be allowed. At 68.4 mT, these two components do coexist, but cannot be clearly distinguished due to the small binding energy of $E_b'=h \times 0.5$ kHz, lower than the experimental resolution of ~ 1 kHz. At 67.6 mT and 66.1 mT, the bound-free transitions are strongly suppressed and the bound-bound transition then shows up as the dominant component in the spectra. The excellent agreement between the experiment and the calculation over a large range of magnetic fields is remarkable. This result strongly suggests that the rf molecular spectroscopy can be used for a precise determination of the atomic interaction parameters [3].

VI. CONCLUSION

We model and evaluate the radio-frequency excitation rates on weakly bound ultracold molecules in the threshold regime. We derive a simple and analytic form of the bound-free and bound-bound spectral profiles which provides an excellent fit to both the numerical calculation and the recent rf measurements on Li_2 molecules.

An interesting case is studied when a Feshbach resonance occurs in the outgoing channel. We show that the bound-free spectra in the absence of a bound state smoothly evolve into a combination of bound-bound and bound-free spectra when a bound state is formed near a Feshbach resonance. The bound-free transition rate strongly depends on the sign of the scattering length and shows a Fano-like structure near the resonance.

We would like to point out that the rf spectroscopy based on ultracold molecules can be a very accurate and excellent tool to determine cold collision properties with high precision. From the excitation spectra, the molecular binding energies, the atomic scattering lengths and their signs, and the scattering phase shifts can be determined [3]. In contrast to photoassociation spectroscopy and collision rate measurements, rf transitions on molecules are insensitive to the sample density and can probe different scattering channels by tuning the rf frequency to different states. Finally, rf transitions between molecular states may also provide a new avenue to transfer the population into low-lying molecular states.

ACKNOWLEDGMENTS

We thank R. Grimm's Li group in Innsbruck for providing the experimental data and stimulating discussions. P.S.J. would like to thank the Office of Naval Research for partial support. C.C. was supported by the Austrian Science Fund (FWF).

[1] C. A. Regal, C. Ticknor, J. L. Bohn, and D. S. Jin, Nature (London) **424**, 47 (2003).
[2] C. Chin, M. Bartenstein, A. Altmeyer, S. Riedl, S. Jochim, J. Hecker Denschlag, and R. Grimm, Science **305**, 1128 (2004).
[3] M. Bartenstein, A. Altmeyer, S. Riedl, R. Geursen, S. Jochim, C. Chin, J. Hecker Denschlag, R. Grimm, A. Simoni, E. Tiesinga, C. J. Williams, and P. S. Julienne, e-print cond-mat/0408673.
[4] P. D. Lett, K. Helmerson, W. D. Phillips, L. P. Ratliff, S. L. Rolston, and M. E. Wagshul, Phys. Rev. Lett. **71**, 2200 (1993); J. D. Miller, R. A. Cline, and D. J. Heinzen, *ibid.* **71**, 2204 (1993).
[5] J. Weiner, S. Zilio, V. Bagnato, and P. S. Julienne, Rev. Mod. Phys. **71**, 1 (1999).
[6] E. R. I. Abraham, W. I. McAlexander, C. A. Sackett, and R. G. Hulet, Phys. Rev. Lett. **74**, 1315 (1995).
[7] G. F. Gribakin and V. V. Flambaum, Phys. Rev. A **48**, 546 (1993).
[8] P. S. Julienne and F. H. Mies, Phys. Rev. A **30**, 831 (1984).
[9] R. Napolitano, J. Weiner, C. J. Williams, and P. S. Julienne, Phys. Rev. Lett. **73**, 1352 (1994); J. Bohn and P. S. Julienne, Phys. Rev. A **60**, 414 (1999).
[10] R. Côté, A. Dalgarno, Y. Sun, and R. G. Hulet, Phys. Rev. Lett. **74**, 3581 (1995).
[11] N. F. Mott and H. S. W. Massey, *The Theory of Atomic Collisions* (Clarendon, Oxford, 1965).

[12] B. Gao, Phys. Rev. A **62**, 050702(R) (2000).
[13] S. Gupta, Z. Hadzibabic, M. W. Zwierlein, C. A. Stan, K. Dieckmann, C. H. Schunck, E. G. M. van Kempen, B. J. Verhaar, and W. Ketterle, Science **300**, 1723 (2003).
[14] Z. C. Yan, J. F. Babb, A. Dalgarno, and G. W. F. Drake, Phys. Rev. A **54**, 2824 (1996).
[15] U. Fano, Phys. Rev. **124**, 1866 (1961).
[16] A. Simoni (private communication). See also Ref. [3].